

DNA Damage-Induced Phosphorylation of TRF2 Is Required for the Fast Pathway of DNA Double-Strand Break Repair[∇]

Nazmul Huda,^{1#} Hiromi Tanaka,^{1#} Marc S. Mendonca,^{1,2} and David Gilley^{1*}

*Department of Medical and Molecular Genetics¹ and Department of Radiation Oncology,²
Indiana University School of Medicine, Indianapolis, Indiana 46202*

Received 13 June 2008/Returned for modification 18 August 2008/Accepted 14 April 2009

Protein kinases of the phosphatidylinositol 3-kinase-like kinase family, originally known to act in maintaining genomic integrity via DNA repair pathways, have been shown to also function in telomere maintenance. Here we focus on the functional role of DNA damage-induced phosphorylation of the essential mammalian telomeric DNA binding protein TRF2, which coordinates the assembly of the proteinaceous cap to disguise the chromosome end from being recognized as a double-strand break (DSB). Previous results suggested a link between the transient induction of human TRF2 phosphorylation at threonine 188 (T188) by the ataxia telangiectasia mutated protein kinase (ATM) and the DNA damage response. Here, we report evidence that X-ray-induced phosphorylation of TRF2 at T188 plays a role in the fast pathway of DNA DSB repair. These results connect the highly transient induction of human TRF2 phosphorylation to the DNA damage response machinery. Thus, we find that a protein known to function in telomere maintenance, TRF2, also plays a functional role in DNA DSB repair.

Telomeres act as protective caps to disguise the chromosome end from being recognized as a DNA double-strand break (DSB) and play other important roles in maintaining genomic integrity (2, 21, 26). Telomere capping dysfunction resulting in genomic instability is likely a major pathway leading to human cancers and other age-related diseases (8, 27).

An increasing number of proteins known to play important roles in DNA repair have also been found to be critical for telomere maintenance (6). Specifically, phosphatidylinositol (PI) 3-kinase-like kinase family members, such as ataxia telangiectasia mutated protein kinase (ATM) and the DNA-dependent protein kinase catalytic subunit in mammals, originally known to act in maintaining genomic stability via DNA repair pathways, have been shown to be important in telomere maintenance (1, 4, 7, 9, 10, 16, 25). Previous reports indicate that ATM is required for the DNA damage-induced phosphorylation of two major telomere-associated proteins in mammals, human TRF1 and TRF2 (16, 28). The specific molecular roles played by the DNA damage-induced phosphorylation of TRF1 and TRF2 in telomere maintenance and/or DNA repair are unclear and under active investigation. We previously reported that upon DNA damage, human TRF2 was rapidly and transiently phosphorylated at threonine 188 (T188) (28). Here, we report that X-ray-induced phosphorylation of human TRF2 at T188 plays a functional role in the fast pathway of DNA DSB repair.

MATERIALS AND METHODS

Construction of TRF2 mutants. Site-directed mutagenesis was performed using Stratagene's QuikChange kit. The MluI and NheI sites were introduced into primer sequences in order to subclone wild-type human TRF2 (TRF2^{WT}) into

pTRE2Hyg (Clontech, CA). Nucleotide sequences of the constructs were checked and confirmed by sequencing both strands. The TRF2 cDNA was provided by Titia de Lange (Rockefeller University, New York, NY).

Cell culture and transfection. HT1080 Tet-Off, advanced MCF7 Tet-Off, and Saos2 Tet-Off cell lines expressing the tetracycline (Tet)-controlled transactivator (tTA) (Clontech) were used. Cells were cultured in advanced Dulbecco's modified Eagle's medium (Invitrogen Inc.) supplemented with L-glutamine, penicillin-streptomycin, 2.5% Tet system-approved fetal bovine serum (Clontech), and 100 µg/ml G418 at 37°C in 5% CO₂. Inducible, high-level gene expression systems for TRF2^{WT} and mutant TRF2 were generated by stably transfecting gene constructs with FuGENE 6 transfection reagent (Roche) into Tet-Off cell lines. The constructs express TRF2^{WT} and mutant TRF2 under the control of a potent Tet-responsive element. The stable transfectants were selected using 200 µg/ml hygromycin. Cells were cultured in the presence of 2 µg/ml of doxycycline (Dox) to repress exogenous TRF2 expression. Fresh Dox was added every 2 days. Dox was removed from the medium to induce exogenous TRF2 overexpression.

Irradiation of cells. Cells were irradiated with 3, 6, or 20 Gy using a 160-kV Faxitron X-ray machine (0.5-mm Cu filter; diameter, 33 cm; dose rate, 64.2 cGy/min) on ice. Irradiated cells were harvested for various times with incubation at 37°C. Mock-irradiated controls were incubated for corresponding times on ice.

shRNA knockdown of TRF2. The short hairpin RNA (shRNA) sequence (leading strand) used for TRF2 gene silencing was GAAGGATCTGGTTCTT CCTACTCAAGCTC (OriGene Technology, Rockville, MD). Transfections were performed using FuGENE HD (Roche). Cells were transfected three times on successive days to produce maximal knockdown.

Clonogenic assay. To measure X-ray sensitivity, clonogenic assays were performed as described previously (18). Cells were induced to express TRF2^{WT} or mutant TRF2 in the absence of Dox for 72 h prior to X-ray treatment and throughout this assay. Control or uninduced cells were continuously grown in the presence of Dox to prevent the expression of exogenous TRF2 alleles. After X-ray treatment, 0.6 × 10³ to 1.5 × 10³ cells were plated on 60-mm dishes. For each sample group, six 60-mm dishes were plated, and the formation of colonies was allowed for 1 week with or without the addition of Dox. Cells were stained with crystal violet and colonies counted to determine the survival fraction of each group. Only colonies with more than 50 cells were counted. Each experiment was repeated three times for each cell line examined. Plating efficiencies for irradiated and unirradiated samples were calculated by dividing the average number of colonies by the number of cells initially plated. Survival fractions were determined by standard methods. To test for significance between surviving fractions obtained in the clonogenic assay, the Student *t* test was performed to assess statistically significant differences between means.

Flow cytometric analysis. An annexin V-enhanced green fluorescent protein apoptosis detection kit was used for the observation of apoptotic cells (Bio-Vision). Cells (5 × 10⁵) were suspended in 0.5 ml of 1× binding buffer. Finally,

* Corresponding author. Mailing address: IB-130, 975 West Walnut Street, Indianapolis, IN 46202. Phone: (317) 278-9158. Fax: (317) 274-1069. E-mail: DPGilley@iupui.edu.

These authors contributed equally to this work.

∇ Published ahead of print on 27 April 2009.

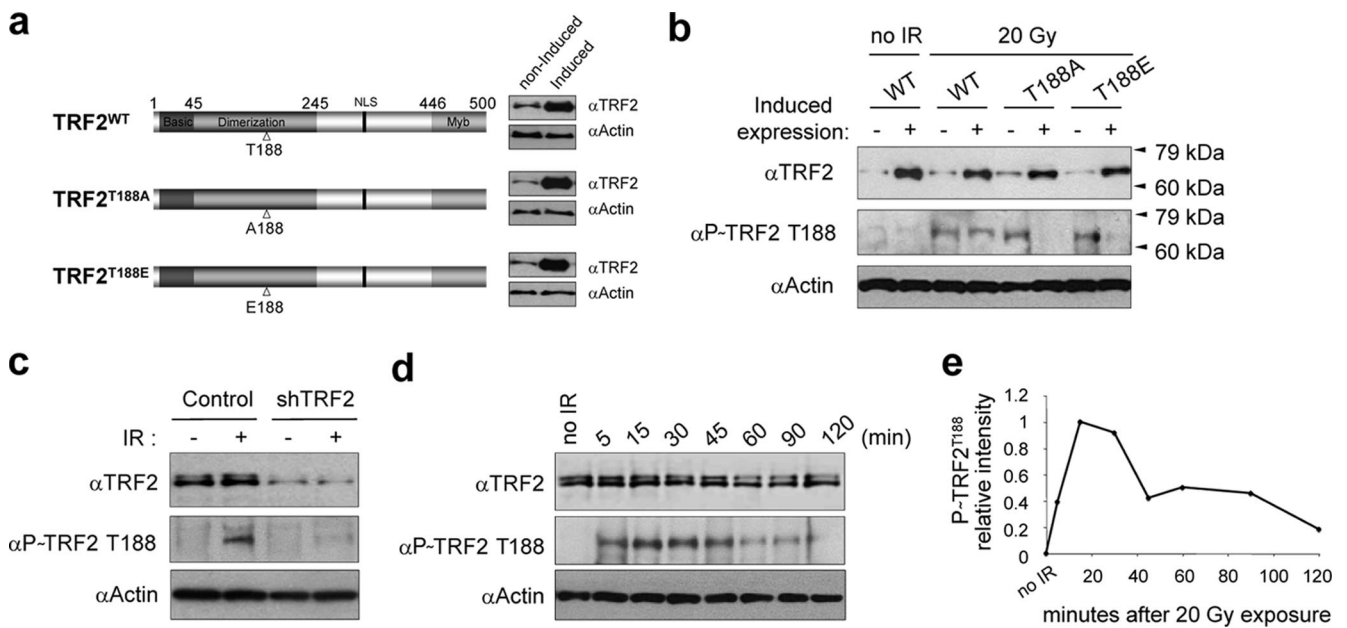


FIG. 1. Overexpression of exogenous TRF2^{T188} mutant protein reduces the levels of endogenous DNA damage-induced P~TRF2^{T188}. For all panels, P~TRF2^{T188} was detected with anti (α)-P~TRF2^{T188} phospho-specific antibody (28); all forms of TRF2 were detected by anti-TRF2 antibody (clone 4A794). (a) Diagram of Tet-inducible TRF2 constructs with mutations at residue T188 and their expression. Exogenous expression of mutant (TRF2^{T188A} and TRF2^{T188E}) and TRF2^{WT} constructs was controlled by the Tet-Off gene expression system in HT1080 cells. Before and after 3 days of induction, cell lysates were analyzed for all forms of TRF2 by immunoblotting. (b) Reduction of endogenous TRF2 phosphorylation by exogenous TRF2^{T188} mutant proteins after ionizing irradiation. To induce exogenous TRF2 constructs, cells were cultured for 3 days without Dox and irradiated (IR) with 20 Gy. Noninduced cells (–) were drugged every 48 h with 2 μg/ml of Dox. (c) Anti-P~TRF2^{T188} is specific for P~TRF2^{T188}. Immunoblotting was performed using cell extract with or without (control) expression of TRF2 shRNA. (d) TRF2^{T188} phosphorylation kinetics after an X ray. Cell were harvested at the indicated time points after 20 Gy of X rays and analyzed by immunoblotting. Antiactin antibody was used as a gel loading control in panels a to d. (e) Graphic representation of P~TRF2^{T188} kinetics.

10 μl of annexin V-enhanced green fluorescent protein and 10 μl of propidium iodide were added, mixed gently, and analyzed by flow cytometry.

Neutral comet assay and single-cell gel electrophoresis. To study DNA DSB repair, neutral comet assays were performed using Comet assay kits (Trevigen). Induced and uninduced cells were prepared and exposed to X rays at 20 Gy on ice. To monitor DSB rejoining, cells were placed at 37°C and trypsinized at different time intervals (0 to 3 h). After being washed with phosphate-buffered saline, the cells were embedded in agarose, lysed, and subjected to neutral electrophoresis. Immediately before image analysis, cells were treated with SYBR green. The cells were examined with a Leica CTR 5000 fluorescence microscope, and comet images were captured using the SPOT RT software. The tail moments of comets were analyzed by the TriTek CometScore Freeware program. Average tail moment values were estimated by examining at least 100 cells per sample.

Immunoblotting and antibodies. Immunoblotting was carried out as previously described (28). We used the following antibodies at the indicated dilutions: anti-TRF2 (1:2,000, 4A794; Imgenex), anti-TRF2 phosphorylated at T188 (anti-P~TRF2^{T188}) (1:500; Millipore/Upstate), anti-H2A (1:1,000, 2572; Cell Signaling Technology), anti-phospho-H2AX (Ser139) (1:2,000, JBW301; Millipore/Upstate), and antiactin (1:10,000, MAB1501; Chemicon International).

Analysis of γ-H2AX foci. Cells were grown in chamber slides in the presence or absence of Dox for 3 days. Cells were exposed to 1 Gy X rays on ice and then cultured at 37°C for 0.5 or 6 h. Cells were stabilized in 0.1 M PIPES [piperazine *N,N'*-bis(2-ethanesulfonic acid)] buffer (pH 6.9) containing 4.0 M glycerol and 1.0 mM EGTA and permeabilized on ice for 5 min in 0.2% Triton X-100. Cells were fixed with formalin solution (Sigma-Aldrich) and blocked twice in 10 mM Tris-HCl buffer (pH 7.5) with 1% bovine serum albumin for 10 min at room temperature. Then cells were incubated with anti-γ-H2AX antibody coupled with fluorescein isothiocyanate (1:200 dilution; Millipore/Upstate) for 1 h at room temperature and washed with 10 mM Tris-HCl buffer (pH 7.5) with 1% bovine serum albumin three times for 10 min each time at room temperature. Cells were mounted with Vectashield mounting medium containing DAPI (4',6-diamidino-2-phenylindole; Victor Laboratories Inc., CA). Fluorescence images were captured using a Leica CTR 5000 fluorescence microscope, and images

were captured using SPOT RT software. At least 55 cells were scored to calculate the number of foci for each sample.

Measurement of telomere length. Genomic DNA was isolated from each cell line, and mean telomere length was measured by in-gel hybridization as described previously (12).

RESULTS

Reduction of endogenous DNA damage-induced P~TRF2^{T188} with overexpression of exogenous TRF2 proteins with a mutation at T188. To investigate the functional consequences of TRF2 DNA damage-induced phosphorylation, we performed a standard disruption and compensatory mutational analysis at TRF2 residue T188 (5, 15). We generated two mutant TRF2 constructs with T188 replaced by alanine (TRF2^{T188A}) or by the phospho-mimic glutamic acid (TRF2^{T188E}) using the inducible Tet-Off expression system (Fig. 1a). We propose that if Thr188 phosphorylation is functionally important, mutant TRF2^{T188A} protein will display a loss of function due to an alanine substitution at this position since this residue cannot be phosphorylated. Alternatively, mutant TRF2^{T188E} protein with a glutamic acid residue at position 188 is expected to restore function by mimicking a constitutively phosphorylated TRF2 at this position (5, 15). Additionally, a TRF2^{WT} construct was also made using the same induction system to determine whether simply overexpressing TRF2^{WT} had a phenotypic effect (Fig. 1a). These three constructs were transfected into the human fibrosarcoma HT1080 Tet-Off cell line, and we isolated stable clones that essentially lacked exogenous TRF2 expres-

sion in the presence of Dox but expressed high levels of exogenous mutant TRF2 or TRF2^{WT} upon removal of Dox from the culture medium (Fig. 1a). We intentionally used non-tagged, exogenously overexpressed TRF2 proteins to avoid potential pitfalls or artifacts due to the addition of tagged residues. We then examined whether overexpression of exogenous TRF2 proteins altered ionizing-radiation-induced phosphorylation of endogenous TRF2 at T188, finding that overexpression of the two mutant TRF2^{T188A} and TRF2^{T188E} proteins, but not of TRF2^{WT}, significantly reduced the amount of X-ray-induced T188 phosphorylation of endogenous TRF2^{WT}, as detected by an anti-P~TRF2^{T188} (phospho-specific) antibody (Fig. 1b) (28). This result suggests that the conditionally overexpressed exogenous mutant proteins (TRF2^{T188A} and TRF2^{T188E}) interfere with or compete for phosphorylation factors, resulting in a reduction in the level of endogenous, X-ray-induced P~TRF2^{T188} (Fig. 1b). To further confirm the phospho specificity of anti-P~TRF2^{T188} antibody, we knocked down endogenous TRF2 levels using shRNA and found a corresponding reduction of signal using the anti-P~TRF2^{T188} antibody (Fig. 1c). Previously, we reported several lines of evidence indicating that this antibody, anti-P~TRF2^{T188}, was specific for DNA damage-induced P~TRF2^{T188} (28). Thus, we additionally demonstrate here that both an overexpression system with specific amino acid changes at T188 (both TRF2^{T188A} and TRF2^{T188E} proteins) and shRNA knockdown of endogenous TRF2 levels correspondingly reduce signal with the anti-P~TRF2^{T188} phospho-specific antibody (Fig. 1b and c). Taken together, these results indicate that this antibody specifically recognizes DNA damage-induced P~TRF2^{T188} under these reported conditions (Fig. 1b and c) (28). As stated above, the amount of X-ray-induced P~TRF2^{T188} protein did not increase even after induction of exogenous TRF2^{WT} (Fig. 1b). This suggests that the amount of DNA damage-induced P~TRF2^{T188} is regulated to a maximum threshold level regardless of increased amounts of steady-state TRF2 protein.

Our previous results demonstrated that the kinetics of the DNA damage-induced appearance of P~TRF2^{T188} was rapid and transient (28). In Fig. 1d, we show that X-ray-induced TRF2 phosphorylation is visible within 5 min but highly transient and that P~TRF2^{T188} is reduced after 1 hour and nearly gone after 2 hours (Fig. 1d and e). These results indicate that X-ray-induced phosphorylation of TRF2 appears to function at early stages of the DNA damage response.

Overexpression of the TRF2^{T188A} mutant protein significantly reduced X-ray survival. To begin investigating whether disruption of the T188 site on TRF2 had functional consequences, we employed a clonogenic X-ray survival assay. We compared levels of X-ray-induced cell killing of cell lines overexpressing mutant TRF2 and TRF2^{WT} that had been irradiated with 3 or 6 Gy. Following irradiation, cells were permitted to recover for 24 h to allow repair and then plated for survival analysis. As important control lines, uninduced TRF2^{T188A} (TRF2^{T188A-}), TRF2^{T188E-}, and TRF2^{WT-} cells were treated every 48 h with 2 μ g/ml of Dox to prevent expression of exogenous TRF2 (Fig. 1b and 2). Three different cell lines were used for this clonogenic survival assay after X-ray treatment, including previously described HT1080 Tet-Off cells along with Saos2 Tet-Off cells (a human osteosarcoma-derived, telome-

rase-independent ALT cell line) and MCF7 Tet-Off cells (a human breast adenocarcinoma [pleural effusion]-derived cell line). Only cells positive for TRF2^{T188A}, predicted to disrupt DNA damage-induced phosphorylation, were more radiation sensitive than the control cells (Fig. 2a, b, and c). Overexpression of the TRF2^{T188A} mutant protein significantly reduced cellular survival compared to that of controls at 3 and 6 Gy (Student's *t* test, $P < 0.005$). We determined that the induced TRF2^{T188A} (TRF2^{T188A+}) line was 30 to 50% more radiation sensitive than control cell lines. To place this reduction of clonogenic survival after X-ray treatment of the TRF2^{T188A+} line in a broader context, we also performed a clonogenic survival assay after X-ray treatment on a cell line deficient for ATM (immortalized fibroblasts from an ataxia telangiectasia patient). Our data indicate that overexpression of the TRF2^{T188A+} mutant protein reduces survival to about one-third of that of ATM-deficient cells, a significant increase in X-ray sensitivity. Importantly, clonogenic survival after X-ray treatment was restored in the cell lines by overexpressing the phospho-mimic glutamic acid mutant construct TRF2^{T188E+} (Fig. 2a, b, and c).

Increased X-ray sensitivity of the TRF2^{T188A} overexpression cell line does not appear to be caused by altered apoptosis or telomere shortening. To explore whether the reduction in X-ray survival of the TRF2^{T188A} overexpression cell line was due to increased apoptotic cell death, we performed a standard annexin V/PI flow cytometry analysis to examine the cell surface phosphatidyl serine apoptotic marker (Fig. 2d) (18a). We found no evidence that apoptosis was significantly altered in the TRF2^{T188A+} cell line compared to that in control lines. In addition, we found that telomere length was essentially unchanged in all cell lines after X-ray exposure (Fig. 2e). In accord with these findings, it was previously reported that irradiation does not alter bulk telomere length in other cell types (24). Therefore, our results and those of others suggest that alterations in telomere length could not explain the increased radiation sensitivity of the TRF2^{T188A+} cell line (24). However, our results do not rule out the possibility that an undetectable amount of critically short telomeres in each cell might cause dysfunction. When our X-ray survival data were plotted as a survival curve, the increased cell killing manifests as a decrease in the slope of the survival curve of the TRF2^{T188A+} line compared to those of control lines (Fig. 2b). A similar change in survival curve shape is observed when DNA repair is inhibited by mutation of various proteins involved in DNA damage sensing and repair (11). These results suggest that phosphorylation of T188 may function in or modulate the DNA damage repair pathway after X-ray exposure.

TRF2^{T188A} expression interferes with the fast pathway of DSB repair. To study whether DNA damage-induced P~TRF2^{T188} plays a role in DNA repair, we performed neutral comet assays to specifically measure DNA DSB repair kinetics after X-ray exposure (23). The repair of DSBs after X-ray exposure has been shown to follow bimodal kinetics with fast and slow repair pathways (14). Under conditions used here, the fast phase of DNA DSB repair occurs within approximately the first hour after DNA damage. This is followed by a switch to a relatively slow phase of DSB repair of several hours, which other investigators have shown to exhibit a higher rate of misjoining or misrepair events (Fig. 3b, uninduced lines) (16a). We found

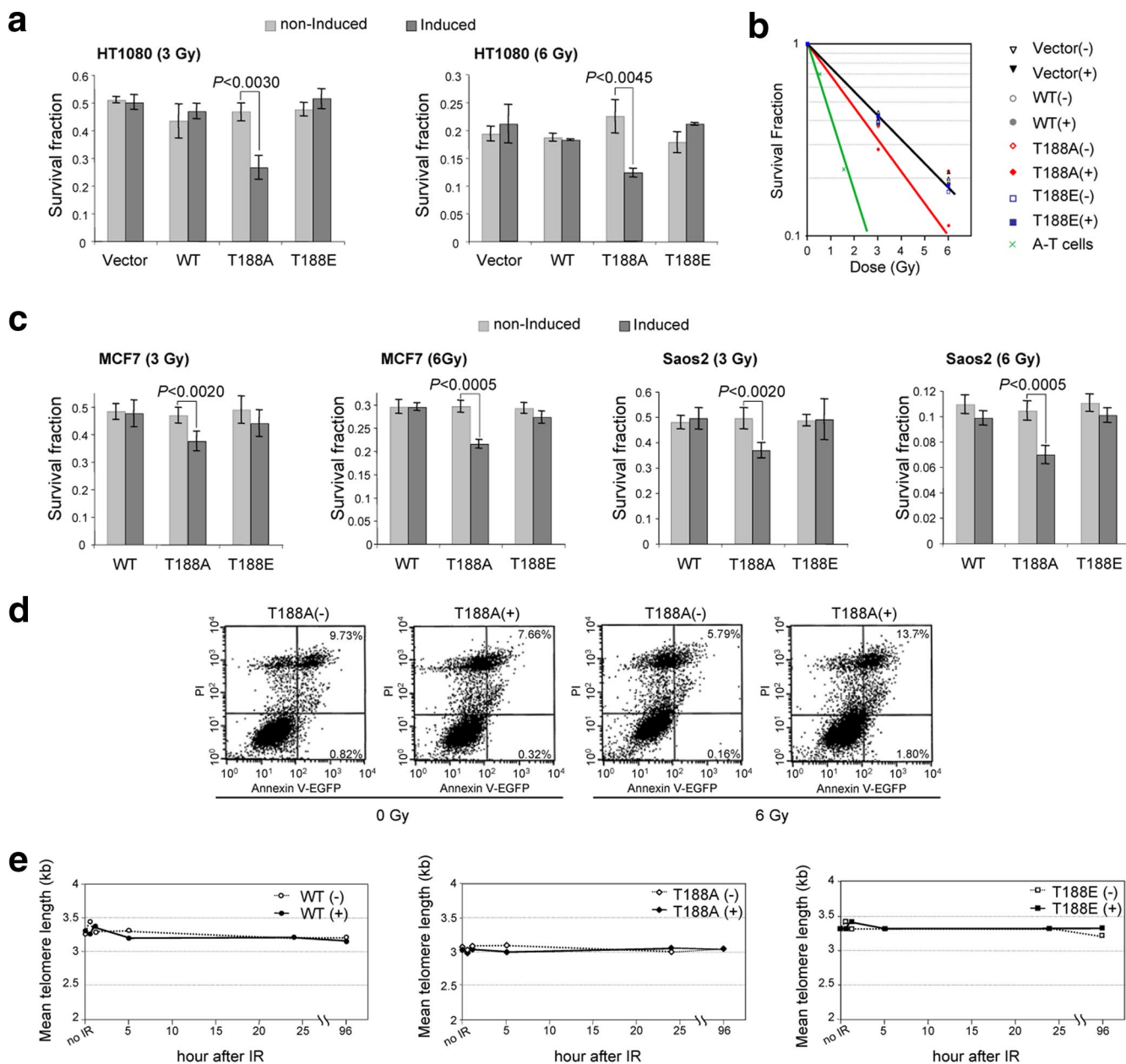


FIG. 2. Overexpression of the TRF2^{T188A} mutant protein significantly reduced survival after X irradiation at 3 and 6 Gy. As described in the text, cells were not induced (-) and induced (+) with exogenous TRF2 constructs. Vector, vector Tet-Off construct only; WT, TRF2^{WT} construct; T188A, TRF2^{T188A}; T188E, TRF2^{T188E}. (a) Histogram of clonogenic survival fractions in HT1080 cells. Cells were treated with 3 or 6 Gy of X-ray exposure. Data are the averages \pm standard deviations (SD) from three independent experiments. (b) Survival curves for HT1080 and immortalized, simian virus 40-transformed ATM cells (A-T cells). Graphical representations of survival fraction data are shown. (c) Histograms of clonogenic survival fractions for MCF7 and Saos2 cells. Cells were treated with 3 or 6 Gy of X-ray exposure. Data are the averages \pm SD of results from three independent experiments. (d) Annexin-V/PI double staining. TRF2^{T188A}-induced (+) and uninduced (-) cells were irradiated with 6 Gy and cultured for 2 days. The percentages shown in the annexin V⁺/PI⁻ and annexin V⁺/PI⁺ regions represent the fractions of cells that died. EGFP, enhanced green fluorescent protein. (e) Quantification of mean telomere length after irradiation (IR). Indicated cell lines were exposed to 20 Gy of X irradiation and harvested after 0, 0.5, 1, 5, 24, and 48 h. Additionally, telomere length did not significantly change during the same harvest times after both 3 and 6 Gy of X-ray exposure (data not shown).

that the fast pathway of DSB repair, occurring within the first hour after X-ray exposure, was essentially eliminated only in cells overexpressing the TRF2^{T188A} mutant protein (Fig. 3a and b). Interestingly, the slope of the results from the slow phase of DNA DSB repair occurring from 1 to several hours after X-ray exposure appeared unaffected in the mutant

TRF2^{T188A} line (Fig. 3b). Uninduced cells containing the TRF2^{T188A} construct and cells containing TRF2^{WT}, either induced or not, efficiently and rapidly repaired DSBs after X-ray exposure (Fig. 3a and b). Importantly, overexpression of the phospho-mimic mutant construct TRF2^{T188E} restored a large portion of the fast pathway of DSB repair (Fig. 3a and b),

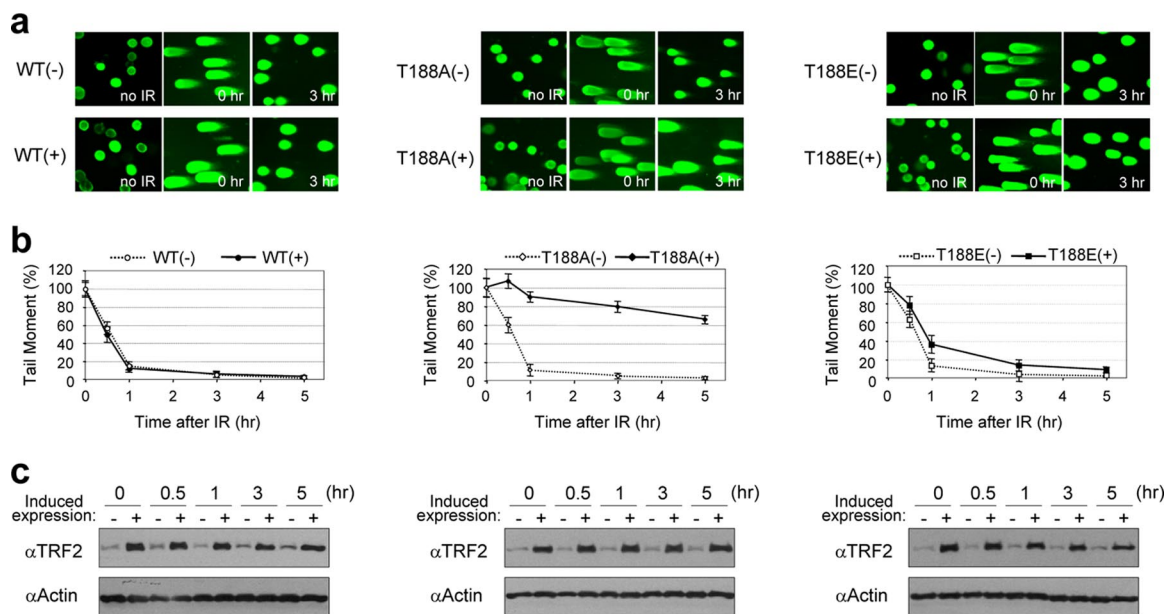


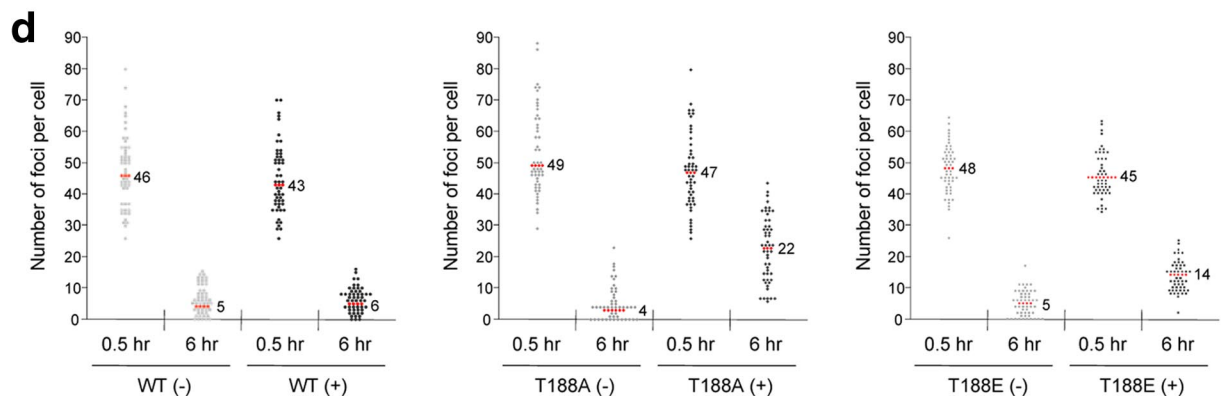
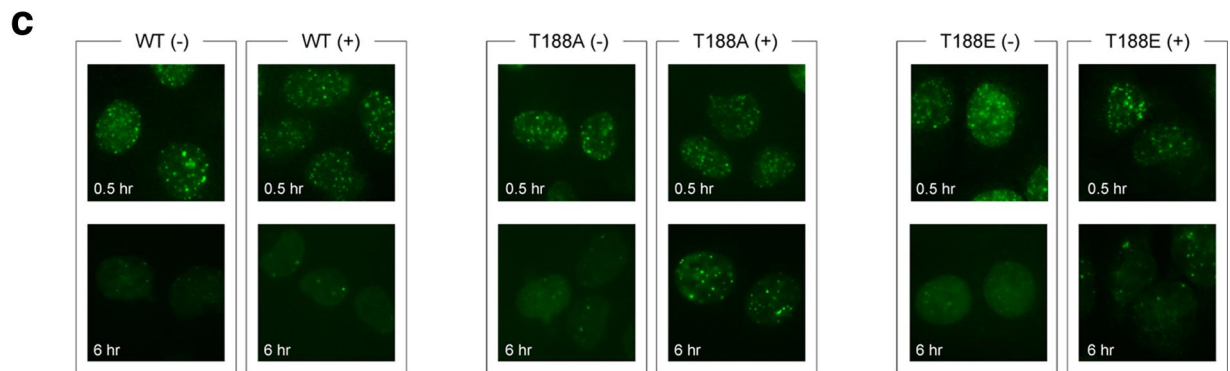
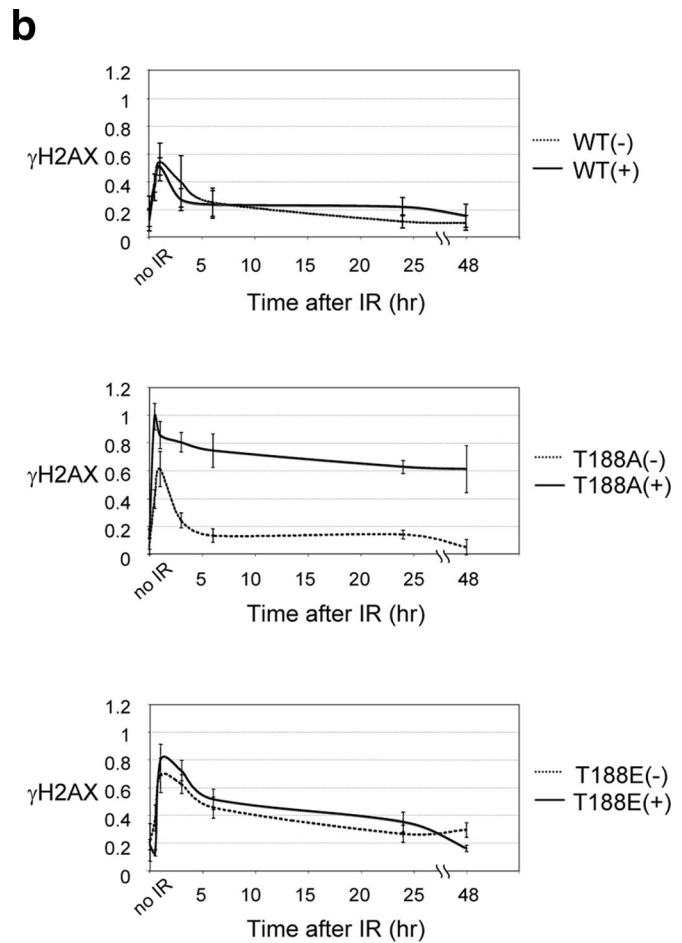
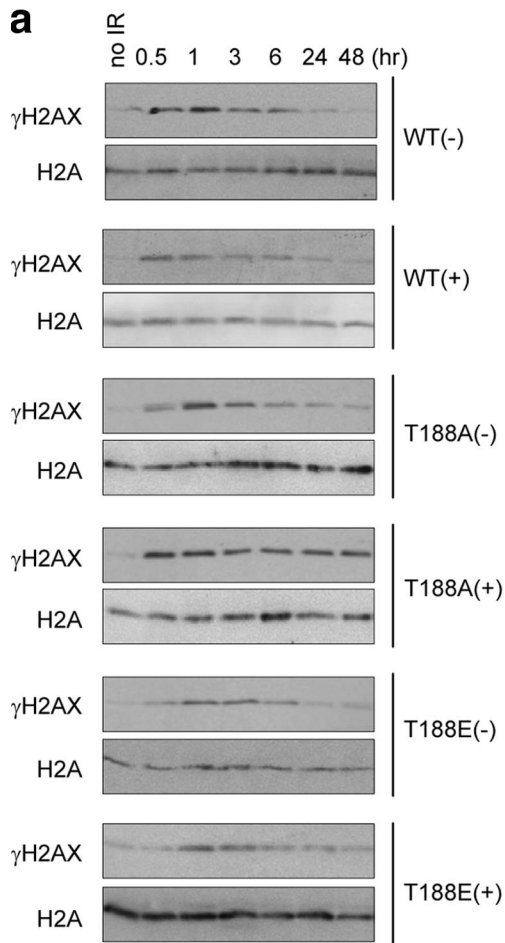
FIG. 3. Phosphorylation of TRF2 at T188 is critical for the fast pathway of DNA DSB repair. Results for cells without induction (-) and with induction (+) of exogenous TRF2 constructs are shown. WT, TRF2^{WT} construct; T188A, TRF2^{T188A}; T188E, TRF2^{T188E}. (a) Representative neutral comet images. Individual cells are shown with no irradiation (IR), just after irradiation (time zero), or 3 h after 20 Gy X-ray exposure. (b) Neutral comet results shown graphically. The graph shows the percentages of tail moment in TRF2^{WT}, TRF2^{T188A}, and TRF2^{T188E} cell lines either without (-) or with (+) overexpression at indicated times after 20 Gy of X irradiation. Comet images were captured by fluorescence microscopy, and the tail moment was analyzed in at least 100 randomly chosen cells by the TriTekCometScore freeware program. The data represent means ± SD. (c) Expression levels of exogenous, inducible TRF2 proteins. Both endogenous and exogenous TRF2 was detected by anti-TRF2 antibody (4A794) from induced (+) and noninduced (-) cell extracts. Antiactin antibody was used as a gel loading control. α, anti.

consistent with our observation that the phospho-mimic mutant protein TRF2^{T188E} does not alter clonogenic survival (Fig. 2a and b). Therefore, the alanine alteration at T188 (TRF2^{T188A}) prevents DNA damage-induced phosphorylation of TRF2 at this position and disrupts the fast pathway DSB repair response. Taken together, our results indicate that the alanine phosphorylation site substitution mutation at TRF2 residue T188 strongly and specifically inhibits the fast pathway of DSB repair after X-ray exposure as determined by the Comet assay (Fig. 3a and b). In contrast, wild-type exogenously overexpressed TRF2 does not affect DSB repair or the amount of steady-state levels of the DNA damage-induced endogenous P~TRF2^{T188}. Therefore, the inhibition of DSB repair observed with the TRF2^{T188A} mutant protein is not likely due to overexpression but appears to be specific to the alanine alteration at T188. These results strongly indicate that phosphorylation of TRF2 at T188 plays an important role in the fast pathway of early DNA DSB repair.

Overexpression of the TRF2^{T188A} protein alters after DNA damage γ-H2AX kinetics. As an early response to DNA damage, the histone H2A variant H2AX is phosphorylated at Ser139 (γ-H2AX) at DNA damage sites and aggregates into foci at sites of DNA DSBs (13). Under conditions used in these experiments, γ-H2AX levels peak at 0.5 to 1 h and then subside by 6 to 10 h after X-ray exposure (Fig. 4a and b) (13). Our neutral comet assay data indicate that substitution of an alanine at residue T188 of TRF2 interferes specifically with the fast but not the slow pathway of DNA DSB repair (Fig. 3). Based on these results, we were interested in whether the kinetics of global γ-H2AX steady-state levels after X-ray exposure

were altered in the TRF2^{T188A} line compared to levels in control lines. Since our results indicated that DNA DSBs persist in TRF2^{T188A} cells, we hypothesized that γ-H2AX levels may also be altered after X-ray exposure, which would be another indication of a DNA repair defect in this line. Indeed, we found that the TRF2^{T188A} line displayed altered γ-H2AX kinetics compared to the kinetics of five control lines exhibiting the highest peak levels approximately 1 hour after X-ray exposure and a subsequent significant delay in the reduction of γ-H2AX steady-state levels (Fig. 4a and b).

Furthermore, we examined the kinetics of DNA damage-induced γ-H2AX nuclear focus formation and disappearance after X-ray treatment. We compared the TRF2^{T188A} line with control lines to determine the median numbers of γ-H2AX nuclear foci at 0.5 and 6 h after 1 Gy X-ray exposure. All cell lines contained similar median numbers of γ-H2AX foci at 0.5 h after X-ray exposure (Fig. 4c and d). In the TRF2^{WT} overexpression cell line and all uninduced cell lines, γ-H2AX focal numbers were greatly reduced 6 h after X-ray exposure (Fig. 4c and d). However, we found that the median number of γ-H2AX foci persisted in the TRF2^{T188A} line 6 h after X-ray exposure, unlike in other cell lines (Fig. 4c and d) (*P* < 0.001). In addition, the TRF2^{T188E} line displayed partial restoration of γ-H2AX nuclear focus disappearance kinetics after X-ray exposure at 6 h compared to the restoration in the TRF2^{T188A} line (Fig. 4c and d) (*P* < 0.001). Therefore, the disruption of DNA damage-induced phosphorylation of TRF2^{T188} due to an alanine substitution alters γ-H2AX steady-state levels and nuclear focal kinetics likely as the result of the continued pres-



ence of DNA DSBs due to a defect in the fast pathway of DNA DSB repair.

DISCUSSION

Previously, we reported that the human telomere-associated protein TRF2 is rapidly and transiently phosphorylated in response to DNA damage by an ATM-dependent pathway (28). Additionally, we found that DNA damage-induced P~TRF2^{T188} is not bound to telomeric DNA, unlike the unphosphorylated form of TRF2, and rapidly accumulates at DNA damage sites (28). Our previous results suggested that DNA damage-induced phosphorylation of TRF2 might play a role in the DNA damage response.

Here, we report that a single alanine substitution at T188 in TRF2 disrupts the fast pathway of DNA DSB repair, reduces clonogenic growth after X-ray treatment, and alters γ -H2AX postdamage kinetics. Importantly, and as expected from previous reports demonstrating that glutamic acid can functionally compensate or mimic a phosphorylated threonine (5, 15), overexpression of the TRF2^{T188E} protein restored clonogenic growth after X-ray treatment and partially restored DNA DSB repair and γ -H2AX postdamage kinetics. Taken together, these results provide strong support that DNA damage-induced phosphorylation of TRF2 at T188 is required for the fast pathway of DNA DSB repair.

We found that both overexpressed TRF2^{T188A} and TRF2^{T188E} mutant proteins suppress the phosphorylation of endogenous P~TRF2^{T188}. The exact cause of this suppression is unknown but is mostly likely due to competition for damage-induced, phosphorylation-dependent factors required by endogenous TRF2. Previous reports indicate that glutamic acid can functionally mimic a phosphorylated threonine or serine likely by restoring residue charge, not local epitope conformation (5, 15). This is consistent with our finding that the anti-P~TRF2^{T188} phospho-specific antibody for the DNA damage-induced form of TRF2 at T188 does not recognize both mutant proteins TRF2^{T188A} and TRF2^{T188E}. Therefore, our results suggest that though overexpression of the phospho-mimic TRF2^{T188E} protein suppresses the phosphorylation of endogenous TRF2, it is able to functionally substitute for phosphorylated TRF2 at residue 188.

We found a corresponding overlap in the kinetics of DNA damage-induced phosphorylation of TRF2 at T188 and disruption of the fast repair of DNA DSBs by overexpression of TRF2^{T188A} (Fig. 1 and 3). Our results suggest that DNA damage-induced TRF2 phosphorylation at T188 occurs and functions during the first hour after DNA damage within the fast

DSB repair pathway. This suggests, based on these early repair kinetics and the work of others, that the phosphorylation of TRF2 at T188 may be involved in the nonhomologous-end-joining pathway (14). While our results do not rule out the possibility that TRF2 protein plays additional roles in DNA repair, our data suggest that DNA damage-induced phosphorylation of TRF2 at T188 functions in the fast pathway of DSB repair via the nonhomologous-end-joining pathway.

Our data indicate that the threshold level of P~TRF2^{T188} is highly regulated and that even increasing exogenous TRF2^{WT} levels did not correspond with increasing levels of DNA damage-induced P~TRF2^{T188}. We propose that a threshold limit of P~TRF2 may prevent the loss of the telomere capping function by TRF2 and may function to precisely control the amount of TRF2 released from the telomere to participate in DNA repair.

Several reports have begun to reveal the involvement of TRF2 in the DNA damage response, in addition to the TRF2 protein's critical role in telomere maintenance (26). These reports suggest that TRF2 (i) is required for the repair of DSBs via the homologous recombination pathway (17), (ii) interacts at nontelomeric sites physically and genetically with several proteins known to function in various pathways of DNA repair (19, 20), (iii) plays an important role in drug resistance (22, 30), and (iv) migrates to DNA damage sites (3, 28). One report repeated previous results regarding TRF2 migration to DNA damage sites using the same damage source as used by Bradshaw et al. (3) but did not observe TRF2 at damage sites using another damage source (29). TRF2 localization at damage sites may be dependent on the specific source or type of DNA damage. Alternatively, TRF2 levels at DNA damage sites may be below the limit of detection for immunofluorescence under certain damage conditions. Regardless, we find that DNA damage-induced P~TRF2^{T188} is critical for DSB repair during early stages after DNA damage and that human TRF2 phosphorylation is highly and unusually transient compared to the phosphorylation of other early DNA damage response proteins by an ATM-dependent signaling pathway.

The exact molecular role that DNA damage-induced P~TRF2^{T188} plays will be an active area of future study. There are several potential mechanistic roles that DNA damage-induced phosphorylation of TRF2 may play in the damage response in the repair of DNA DSBs. One possibility is that DNA damage-induced phosphorylation of TRF2 either facilitates or disrupts a specific protein-protein interaction potentially at the sites of DNA DSBs. In addition, DNA damage-induced phosphorylation of TRF2 at T188 may be required to

FIG. 4. TRF2^{T188A} protein alters after DNA damage γ -H2AX kinetics. Cells without induction (–) and with induction (+) of exogenous TRF2 proteins. WT, TRF2^{WT} construct; T188A, TRF2^{T188A}; T188E, TRF2^{T188E}. (a) Western analysis of γ -H2AX kinetics. Extracts for each cell line were collected at 0.5, 1, 3, 6, 24, and 48 h after 6 Gy of X irradiation (IR) exposure and analyzed by immunoblotting with antibodies against γ -H2AX and H2A. (b) Graphic representations of relative γ -H2AX levels after DNA damage. Immunoblotting levels from three independent experiments were quantified by gel densitometry. Relative γ -H2AX levels were first normalized within each cell line to endogenous H2A levels. Additionally, we compared γ -H2AX levels between all cell lines for final normalization. The highest level of γ -H2AX was set to a maximum relative level of 1.0. The means \pm SD are shown. (c) Representative images of γ -H2AX foci. Cells were seeded onto chamber slides, irradiated with 1 Gy of X irradiation, cultured for 0.5 or 6 h, fixed, and stained for γ -H2AX. (d) Quantitative analysis of γ -H2AX foci. γ -H2AX foci were scored in a blind manner, and the number of foci per nucleus was plotted. Fifty-five samples were used for each cell line at each time point. The median numbers of foci/nucleus are shown numerically and as red dots.

facilitate the dissociation of TRF2 from the telomere to sites of DNA damage.

Our results indicate that P~TRF2^{T188} is required for or modulates the fast pathway of DSB repair. Experimental results presented here and previously (3, 28), along with results from others showing that TRF2 performs roles in the DNA damage response (17, 19, 20, 22, 30), strongly suggest that TRF2 functions at DNA DSBs and that DNA damage-induced phosphorylation of TRF2 may facilitate its localization to these damage sites. Additionally, DNA damage-induced phosphorylation of TRF2 may function to allow TRF2 to perform a direct role as a mediator or effector in the DNA damage response.

ACKNOWLEDGMENTS

We thank John Turchi for assistance in performing the Comet assay analysis. We thank Anna Malkova, John Turchi, and Junya Kobayashi for valuable comments during the preparation of the manuscript. We thank Helen Chin-Sinex for valuable technical support during X-ray exposures.

This work was supported by the Indiana University Cancer Center, the American Cancer Society, the Showalter Foundation, the Susan G. Komen Foundation, the Avon Foundation, and the Indiana Genomics Initiative (INGEN). INGEN of Indiana University is supported in part by Lilly Endowment Inc.

REFERENCES

- Bailey, S. M., J. Meyne, D. J. Chen, A. Kurimasa, G. C. Li, B. E. Lehnert, and E. H. Goodwin. 1999. DNA double-strand break repair proteins are required to cap the ends of mammalian chromosomes. *Proc. Natl. Acad. Sci. USA* **96**:14899–14904.
- Blackburn, E. H. 2001. Switching and signaling at the telomere. *Cell* **106**:661–673.
- Bradshaw, P. S., D. J. Stavropoulos, and M. S. Meyn. 2005. Human telomeric protein TRF2 associates with genomic double-strand breaks as an early response to DNA damage. *Nat. Genet.* **37**:193–197.
- Denchi, E. L., and T. de Lange. 2007. Protection of telomeres through independent control of ATM and ATR by TRF2 and POT1. *Nature* **448**:1068–1071.
- Downs, J. A., N. F. Lowndes, and S. P. Jackson. 2000. A role for *Saccharomyces cerevisiae* histone H2A in DNA repair. *Nature* **408**:1001–1004.
- Genescà, A., M. Martín, L. Latre, D. Soler, J. Pampalona, and L. Tusell. 2006. Telomere dysfunction: a new player in radiation sensitivity. *Bioessays* **28**:1172–1180.
- Gilley, D., H. Tanaka, M. P. Hande, A. Kurimasa, G. C. Li, M. Oshimura, and D. J. Chen. 2001. DNA-PKcs is critical for telomere capping. *Proc. Natl. Acad. Sci. USA* **98**:15084–15088.
- Gilley, D., B. S. Herbert, N. Huda, H. Tanaka, and T. Reed. 2008. Factors impacting human telomere homeostasis and age-related disease. *Mech. Ageing Dev.* **29**:27–34.
- Goytisolo, F. A., E. Samper, S. Edmonson, G. E. Taccioli, and M. A. Blasco. 2001. The absence of the DNA-dependent protein kinase catalytic subunit in mice results in anaphase bridges and in increased telomeric fusions with normal telomere length and G-strand overhang. *Mol. Cell. Biol.* **21**:3642–3651.
- Hande, M. P., A. S. Balajee, A. Tchirkov, A. Wynshaw-Boris, and P. M. Lansdorp. 2001. Extra-chromosomal telomeric DNA in cells from *Atm*^{-/-} mice and patients with ataxia-telangiectasia. *Hum. Mol. Genet.* **10**:519–528.
- Harper, J. W., and S. J. Elledge. 2007. The DNA damage response: ten years after. *Mol. Cell* **28**:739–745.
- Huda, N., H. Tanaka, B. S. Herbert, T. Reed, and D. Gilley. 2007. Shared environmental factors associated with telomere length maintenance in elderly male twins. *Ageing Cell* **6**:709–713.
- Huen, M. S., and J. Chen. 2008. The DNA damage response pathways: at the crossroad of protein modifications. *Cell Res.* **18**:8–16.
- Iliakis, G., H. Wang, A. R. Perrault, W. Boecker, B. Rosidi, F. Windhofer, W. Wu, J. Guan, G. Terzoudi, and G. Pantelias. 2004. Mechanisms of DNA double strand break repair and chromosome aberration formation. *Cytogenet. Genome Res.* **104**:14–20.
- Kauppinen, T. M., W. Y. Chan, S. W. Suh, A. K. Wiggins, E. J. Huang, and R. A. Swanson. 2006. Direct phosphorylation and regulation of poly(ADP-ribose) polymerase-1 by extracellular signal-regulated kinases. *Proc. Natl. Acad. Sci. USA* **103**:7136–7141.
- Kishi, S., X. Z. Zhou, Y. Ziv, C. Khoo, D. E. Hill, Y. Shiloh, and K. P. Lu. 2001. Telomeric protein Pin2/TRF1 as an important ATM target in response to double strand DNA breaks. *J. Biol. Chem.* **276**:29282–29291.
- Löblich, M., B. Rydberg, and P. K. Cooper. 1995. Repair of X-ray-induced DNA double-strand breaks in specific Not 1 restriction fragments in human fibroblasts: joining of correct and incorrect ends. *Proc. Natl. Acad. Sci. USA* **92**:12050–12054.
- Mao, Z., A. Seluanov, Y. Jiang, and V. Gorbunova. 2007. TRF2 is required for repair of nontelomeric DNA double-strand breaks by homologous recombination. *Proc. Natl. Acad. Sci. USA* **104**:13068–13073.
- Mendonça, M. S., C. Sun, and J. L. Redpath. 1990. Suppression of radiation-induced neoplastic transformation of human cell hybrids by long term incubation at low extracellular pH. *Cancer Res.* **50**:2123–2127.
- Mendonça, M. S., H. Chin-Sinex, J. Gomez-Millan, N. Datzman, M. Hardacre, K. Comerford, H. Nakshatri, M. Nye, L. Benjamin, S. Mehta, F. Patino, and C. Sweeney. 2007. Parthenolide sensitizes cells to X-ray-induced cell killing through inhibition of NF-kappaB and split-dose repair. *Radiat. Res.* **168**:689–697.
- Muftuoglu, M., H. K. Wong, S. Z. Imam, D. M. Wilson III, V. A. Bohr, and P. L. Opresko. 2006. Telomere repeat binding factor 2 interacts with base excision repair proteins and stimulates DNA synthesis by DNA polymerase beta. *Cancer Res.* **66**:113–124.
- Munoz, P., R. Blanco, J. M. Flores, and M. A. Blasco. 2005. XPF nuclease-dependent telomere loss and increased DNA damage in mice overexpressing TRF2 result in premature aging and cancer. *Nat. Genet.* **37**:1063–1071.
- Murnane, J. P., and L. Sabatier. 2004. Chromosome rearrangements resulting from telomere dysfunction and their role in cancer. *Bioessays* **26**:1164–1174.
- Ning, H., T. Li, L. Zhao, T. Li, J. Li, J. Liu, Z. Liu, and D. Fan. 2006. TRF2 promotes multidrug resistance in gastric cancer cells. *Cancer Biol. Ther.* **5**:957–958.
- Olive, P. L. 2009. Impact of the comet assay in radiobiology. *Mutat. Res.* **681**:13–23.
- Serakinci, N., R. Christensen, J. Graakjaer, C. J. Cairney, W. N. Keith, J. Alsner, G. Saretzki, and S. Kolvraa. 2007. Ectopically hTERT expressing adult human mesenchymal stem cells are less radiosensitive than their telomerase negative counterpart. *Exp. Cell Res.* **313**:1056–1067.
- Smilenov, L. B., S. E. Morgan, W. Mellado, S. G. Sawant, M. B. Kastan, and T. K. Pandita. 1997. Influence of ATM function on telomere metabolism. *Oncogene* **15**:2659–2665.
- Smogorzewska, A., and de T. Lange. 2004. Regulation of telomerase by telomeric proteins. *Annu. Rev. Biochem.* **73**:177–208.
- Stewart, S. A., and R. A. Weinberg. 2006. Telomeres: cancer to human aging. *Annu. Rev. Cell Dev. Biol.* **22**:531–557.
- Tanaka, H., M. S. Mendonça, P. S. Bradshaw, D. J. Hoelz, L. H. Malkas, M. S. Meyn, and D. Gilley. 2005. DNA damage-induced phosphorylation of the human telomere-associated protein TRF2. *Proc. Natl. Acad. Sci. USA* **102**:15539–15544.
- Williams, E. S., J. Stap, J. Essers, B. Ponnaiya, M. S. Luijsterburg, P. M. Krawczyk, R. L. Ullrich, J. A. Aten, and S. M. Bailey. 2007. DNA double-strand breaks are not sufficient to initiate recruitment of TRF2. *Nat. Genet.* **39**:696–699.
- Zhang, Y. W., Z. X. Zhang, Z. H. Miao, and J. Ding. 2008. The telomeric protein TRF2 is critical for the protection of A549 cells from both telomere erosion and DNA double-strand breaks driven by salivicine. *Mol. Pharmacol.* **73**:824–832.